

Effects of Atomic N Adsorption on Electronic Structures of MgO (001) Surface

Li-Min Fang, Ke-Lun Zhao

*Corresponding author email id: klzhao1975@163.com

Date of publication (dd/mm/yyyy): 09/01/2017

Abstract – The adsorption effects of atomic N on atomic configurations, bonding characteristics, and electronic structures of MgO(001) surface are investigated by performing the plane-wave pseudopotential calculations within the density functional theory. After structure optimizations, it is found that not only the stability of N but the surface distortions are deeply dependent on the relative position of the adsorbed N atom to the surface. Based on the analysis of energy band structures, projected densities of states and electron densities difference of the surface atoms, it is revealed that the N-induced electron states are closely related to electron transfer from the adsorbed N to the surface. Our results suggest that atomic N adsorption would improve the catalytic activity of pure MgO(001) surface.

Keywords – Electronic Structure, Atomic Adsorption.

I. INTRODUCTION

Nitrogen (N) doping of oxides materials have been paid to much attention in recent years because of its extensive application in the field of photocatalysts, remediation and solar energy conversion [1-4]. Along with the various oxide materials mentioned above, N-doped MgO is also receiving extensive research interests due to its functional application in potential spintronics devices [5-8]. Experimentally, Liu et al. [5] reported that the nitrogen doping is considered to be the main origin of ferromagnetism from the microstructure, optical property and magnetism of nitrogen ion implanted MgO single crystals. Theoretically, Nickel et al. [6] has found that the appearance of the localized gap states is caused by N₂ molecule incorporation into bulk MgO. Afterwards, Pacchioni et al. [7] investigated the defect nature of nitrogen-doped bulk MgO, which indicates that both substitutional and interstitial N introduce magnetic impurities in bulk MgO and generate new energy levels at about 0.5-1.7 eV above the top of the MgO valence band. Additionally, Kim et al. [8] have explored the magnetic properties of ultrathin C and N layers on MgO(001) surface, which shows that the free standing C layer has a ferromagnetic (FM) ordering, while the free standing N layer with the same coverage displays an antiferromagnetic (AFM) state. In general, the presence of nitrogen adsorbates on oxide surfaces would influence the defect formation, surface reconstruction, and chemical reactions at the surface. For instance, atomic nitrogen adsorption on the TiO₂(110) and SrTiO₃(001) surfaces would give rise to both remarkable surface distortions and the significant change of electronic properties [9, 10]. To the best of our knowledge, there is very little theoretical investigation on N-adsorbed MgO(001) surfaces so far. In the present work, the adsorption effects of atomic N on the atomic configurations, bonding characteristics, and electronic structures of

MgO(001) surface are studied by using the plane-wave pseudopotential calculations based on the density functional theory.

II. COMPUTATIONAL DETAILS

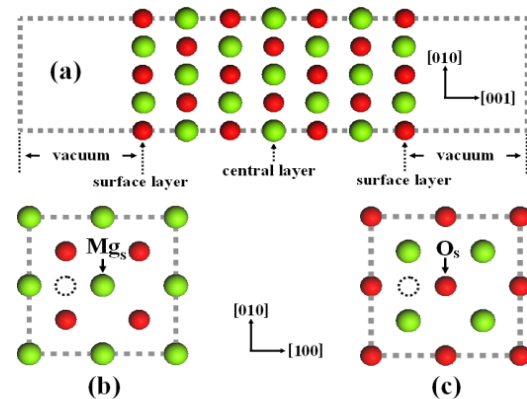


Fig. 1. Schematics of the computational cell for the N-adsorbed MgO(001) surfaces. (a) is the side view of the surfaces; (b) and (c) display the atomic structure of the (001)MgO surface layers. The green and red spheres are corresponding to Mg and O atoms, and the different adsorption sites (Mgs, Os and interstice) on the surface layer are marked by the black arrows and dash circles.

First-principles calculations have been successfully used in the microscopic understanding of the structural and electronic properties of MgO surfaces [11, 12]. In the present study, the plane-wave pseudo-potential(PWPP) calculations are performed within the density functional theory by using the CASTEP code [13]. The generalized gradient approximation (GGA) was used for all the atomic calculations and the formation of the pseudo-potentials[14, 15]. The most frequently used functional form of the GGA is PW91 [16], which have been proven to be well working [17]. The MgO(001) surface system was represented by 2×2 supercell models with three-dimensional periodicity as schematically illustrated in Fig. 1(a), in which the slab of MgO(001) surface was consisting of seven atomic layers with alternating atomic planes as shown in Figs. 1(b) and 1(c). Fig. 1(a) shows the atomic structure of pure MgO(001) surface and the N-adsorbed surfaces are defined by the different N adsorption sites (Mgs, Os, and interstice (dashed circle)) on the surface layer, respectively, as displayed in Figs. 1(b) and 1(c). Furthermore, it should be pointed out that MgO(001) surface slabs with seven atomic layers were large enough to describe the electronic structures of atomic adsorption on MgO(001) surfaces [11]. Moreover, the 2×2 MgO(001) surface supercell is labeled by the mirror-symmetrical slabs with the central layer, in which the

surface slab is sandwiched by two vacuum layers (14 Å), the thickness of which sufficiently is large to avoid spurious interactions between the periodic images of the supercell perpendicular to the surfaces [12]. In the present calculations, the plane-wave energy cutoff is set to 350 eV. The 6×6×1 Monkhorst-Pack k-point meshes [18] are used in the Brillouin zone integration. All the atoms in each supercell are relaxed until the total energy difference between two steps is smaller than 1×10⁻⁵ eV/atom. The total energy is minimized by means of a conjugate gradient technique [19]. The Vanderbilt ultrasoft pseudopotentials [20] of different types of atoms in each supercell are taken to determine the appropriate plane-wave basis set. The density-mixing scheme based on the Pulay algorithm [21] is used for self-consistent-field (SCF) calculation, in which the SCF tolerance is set at 1×10⁻⁶ eV/atom. After geometry optimizations, the remaining forces on the atoms are less than 0.03 eV/Å, and the remaining stress is less than 0.05 GPa. For a consistent comparison, all of the MgO(001) surface supercells have been fully relaxed, not only in the vertical direction but also within lateral relaxation of atoms.

Table 1. Lattice constants a_0 , bulk modulus B_0 and band gap of MgO according to earlier experiments and recent calculations based on various methods.

Methods	a_0 (Å)	B_0 (GPa)	Band Gap (eV)	References
Experiment.	0.4210	160	7.83	22, 23
FP-KKR ^a	0.4248	153		24
TB-LMTO ^b	0.4160		5.20	25
FP-LAPW ^c	0.4165	171	5.00	26
PWPP-GGA	0.4301	177	4.94	This study

^aFull potential Korringa-Kohn-Rostoker Green's function

^bTight-Binding Linear muffin-tin orbital method

^cFull potential linear augmented plane-wave method

To examine the above-mentioned parameters, we first employed the PWPP-GGA method to calculate the structural properties for bulk MgO. Table 1 lists the calculated and experimental lattice constants, bulk modulus, and band gaps of bulk MgO. The calculated crystal lattice constants and bulk modulus agree well with the experimental [22-23] and other theoretical values [24-26], although our calculated band gap of bulk MgO (4.94 eV) is much less than the experimental value (7.83 eV) which is typical for DFT calculations. Accordingly, in this work, the PWPP-GGA calculations within the density functional theory are performed to investigate the electronic structures of N-adsorbed MgO(001) surfaces.

III. RESULTS AND CONCLUSIONS

For the N-adsorbed MgO(001) surfaces, the adsorption energy of N, E_{ads} , can be calculated by

$$E_{ads} = E_{N-ads} - E_{Perfect} - \frac{1}{2} E(N_2) \quad (1)$$

where E_{N-ads} and $E_{Perfect}$ are the total energies of N adsorption and perfect surface supercell after structure optimizations, respectively. $E(N_2)$ is the total energy of an isolated N_2 molecule. In Eq. (1), the adsorption energy E_{ads} is defined

negative for the adsorbed N atom on the MgO(001) surface. As we know the shortcoming of the density functional theory method tends to overestimate binding energies. Accuracy of binding energies depends on the choice of the exchange and correlation functional, leading to discrepancies in absolute values. In the present study, we are interested in the qualitative trends of the adsorption and substitution energies, and not in absolute values, therefore not interfering in the main conclusions of this work. Table 2 lists the adsorption energies and the distances between the adsorbed N atom and different adsorption sites on the surface layer. For the adsorbed N on MgO(001) surface, interstice site is the most stable site since it has the highest adsorption energy and the smallest distance. Besides, it is worth noting that O_s are more favorable sites than Mg_s, which implies that the adsorbed N atom would like to bond to O atom on the surface.

Table 2. Adsorption energies (E_{ads}) and atomic distances (D_s) between the adsorbed N and different adsorption sites on MgO(001) surface after structure optimizations.

Models	Adsorption Sites (#)	E_{ads} (eV/atom)	D_s (Å) (N and #)
B	Mg	-0.48	2.06
C	O	-1.35	1.48
D	Interstice	-1.69	1.12

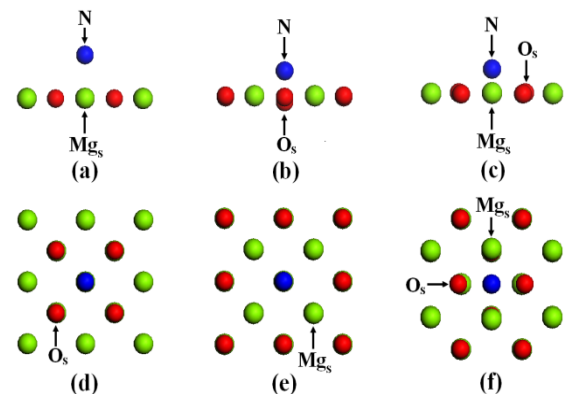


Fig. 2. Optimized atomic structures of the N-adsorbed MgO(001) surface, in which (a), (b), and (c) are the side view of the N adsorbed on Mg_s, O_s and interstice on the surface only shown in the surface layers respectively; while (d), (e), and (f) are the top view of the N adsorbed on different adsorption sites corresponding to (a), (b), and (c), only displayed in two atomic layers of MgO(001) surface, respectively.

Fig. 2 shows the optimized structures of the N-adsorbed MgO(001) surface. It is clearly shown that the presence of the adsorbed N on the surface causes the surface distortions in different degrees. For the adsorbed N on Mg_s in Figs. 2(a) and 2(d), it is seen that there is no obvious surface distortions, while the distance (2.06 Å) between N and Mg_s is much larger than that (1.48 Å (1.12 Å)) between N and O_s (interstice) in Figs. 2(b) and 2(c). For the adsorbed N on O_s in Figs. 2(b) and 2(e), it can be found that the O_s atom deviates from the surface layer and moves down along the [001] direction, which result in the distance (1.48 Å)

between N and O_s is little larger than that (1.48 Å) between N and interstice in Fig. 2(c). For the adsorbed N on interstice in Figs. 2(c) and 2(f), it is observed that the nearest two O_s(Mg_s) atoms of the interstice are slightly displaced away from the interstice site, which implies that the adsorbed N will interact with both two O_s (Mg_s) atoms on the surface. Therefore, all of above make the interstice more favorable site for the adsorbed N than other adsorption sites on MgO(001) surface.

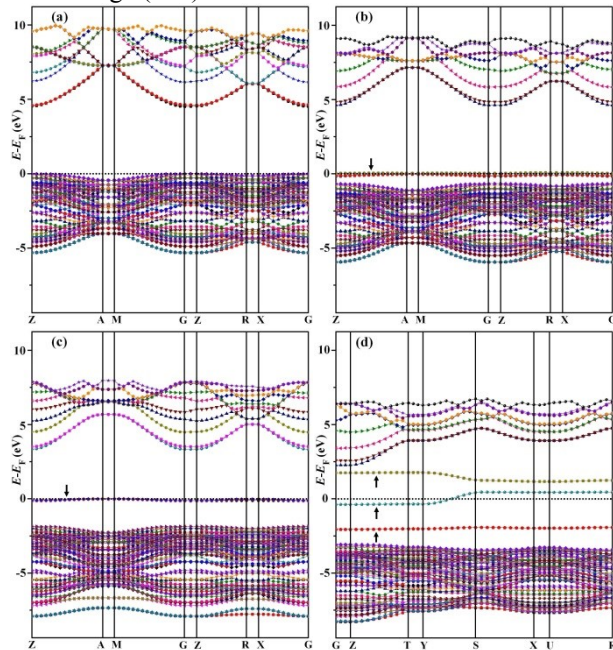


Fig. 3. Band structure of MgO(001) surfaces with and without atomic N adsorptions. Herein, (a) stands for pure surface; (b), (c), and (d) are the N-adsorbed surfaces corresponding to different adsorption sites (Mg_s, O_s and interstice) on the surface layer, respectively. Note that N-induced electron states are denoted by black arrows, and the Fermi energy level is represented by the black dot-line.

To understand the fundamental properties of the N-adsorbed surface, Fig. 3 presents the band structure of the pure and N-adsorbed MgO(001) surfaces. For the pure surface in Fig. 3(a), it can be seen that the top of the valence bands is at the Z point of the Brillouin zone, which mainly comes from the 2p orbitals of the surface oxygen atoms. The two lowest conduction bands are degenerate at the Z point of the Brillouin zone, which are predominantly contributed by the 2p orbitals of the surface oxygen atoms and 2s, 2p orbitals of the surface Mg atoms. Therefore, the direct band gap of pure MgO(001) surface will be about 4.53 eV since there are no surface distortions in the pure surface (not shown in this paper). These characteristics of band structures for pure MgO(001) surface agree well with bulk MgO [25, 26], although the band gap of pure MgO(001) surface is less than that (4.94 eV) of bulk MgO listed in Table 1.

For the surface with N adsorbed on Mg_s in Fig. 3(b), the most important characteristic is that atomic N adsorption causes two narrow hybrid bands just across the Fermi level, while there is almost no change in the conduction band structures. This is because that in this case the structural

distortion caused by N adsorption is very small as shown in Figs. 2(a) and 2(d). However, it is notable that the two lowest conduction bands become nondegenerate at the Z point of the Brillouin zone as compared with the pure surface. In addition, the band gap in this case is 4.49 eV just little less than that (4.53 eV) of the pure surface, which indicates that the electronic properties of MgO(001) surface with N adsorption on the surface Mg atoms is very similar with that of the pure surface.

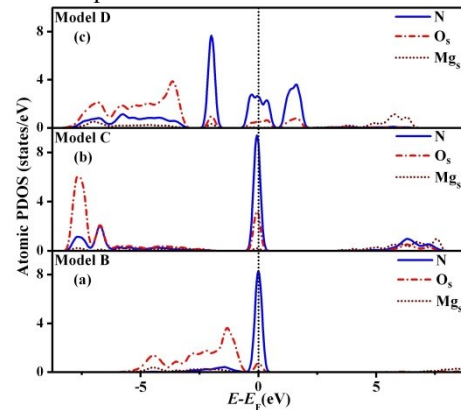


Fig. 4. PDOSs of different atoms on the surface layer in the N-adsorbed MgO(001) supercells, where (a), (b), and (c) are corresponding to the different adsorption sites (Mg_s, O_s and interstice) on the surface layer, respectively.

For the surface with N adsorbed on O_s in Fig. 3(c), it is also clearly observed that two narrow hybrid bands with 2p character of N and O_s appear right across the Fermi level, while the two lowest conduction bands become nondegenerate at the Z point of the Brillouin zone. Moreover, it should be noticed that the presence of two narrow hybrid bands in the valence bands region (around -7.5 eV), which mainly come from 2p orbital of the adsorbed N and O_s with the vertical movement into the surface layer as shown in Fig. 2(b), suggests that the hybridization effects in valence bands between 2p orbital electrons of the adsorbed N and O_s atoms would become stronger than that of the pure surface. All of above makes the band gap (3.46 eV) in this case much less than that of the pure surface, which could lead to change in the insulating nature of the pure surface, such as the photocatalytic activity of MgO film [11, 12].

For the surface with N adsorbed on the interstice in Fig. 3(d), it can be found that the total band structures are very different from that of the other surfaces. This is because in this case that atomic N adsorption leads to obvious change in not only the structural symmetry of this system but also the atomic configuration of the surface as displayed in Fig. 2(c) and (f). More importantly, it is worth noting that there are three narrow hybrid bands around the Fermi level, predominantly contributed by hybridization interactions between 2p orbital electrons of the adsorbed N and two O_s atoms on the surface layer, which means that in this case the surface could become metallic in contrast to that of the pure surface.

To further explore the electronic structures of the N-adsorbed surface, Fig. 4 shows the calculated projected density of states (PDOSs) of the surface atoms. For the

surface with N adsorbed on Mg_s in Fig. 4(a), it is seen that the very sharp peak of the N $2p$ states just around the Fermi level is coincide with the weak peak of the O_s $2p$ states, which implies that the hybridization effects between the $2p$ states of N and O_s result in the appearance of two narrow bands just across the Fermi level as presented in Fig. 3(b).

For the surface with N adsorbed on O_s in Fig. 4(b), it is also found that the very sharp peak of the N $2p$ states is corresponding to the stronger peak of the O_s $2p$ states around the Fermi level, which leads to the presence of two narrow bands just across the Fermi level as displayed in Fig. 3(c). Meaning while, it is obvious that two hybridization peaks between the $2p$ states of N and O_s appear around -7.5 eV, which are consistent with the two narrow hybrid bands in the valance band region in Fig. 3(c). For the surface with N adsorbed on the interstice in Fig. 4(c), it is notable that there are three hybridization peaks between the $2p$ states of N and O_s in the energy region from -3.5 eV to 2.5 eV, which are in agreement with the band structures around the Fermi level as marked in Fig. 3(d). Furthermore, it should be noticed that the hybridization effects between $2p$ electron states of N and O_s atoms in the energy region from -8.0 eV to 2.0 eV increases in sequence from $N_{ads}-Mg_s$ to $N_{ads}-O_s$ and then N_{ads} -interstice, which agrees well with the trend of the adsorption energies of N on different adsorption sites listed in Table 2.

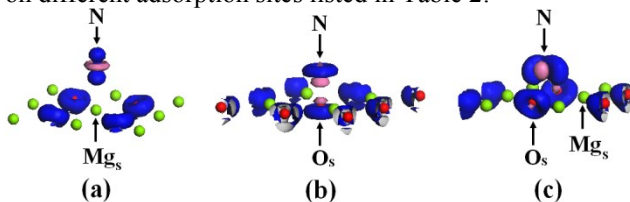


Fig. 5. Electron density difference of the surface atoms in N-adsorbed MgO(001) supercells, in which (a), (b), and (c) correspond to the different adsorption sites (Mg_s , O_s and interstice) on the surface layer, respectively.

The isosurfaces at the value of $0.14 \text{ e}/\text{\AA}^3$ and $-0.14 \text{ e}/\text{\AA}^3$ are depicted by the blue and pink contours, respectively, which represent the electron accumulation and depletion regions around the surface atoms, respectively. The green and red spheres are corresponding to Mg and O atoms, respectively, in the same as those shown in Fig. 1.

To better understand the effects of N adsorption on electronic structures of MgO(001) surface, we calculated the electron density difference of the surface atoms as shown in Fig. 5. It is clearly observed in the three cases that both the depletion and accumulation regions of orbital electrons are all around the adsorbed N atom on the surface, but the electron redistribution of the surface O atoms are very different from each other. For the surface with N adsorbed on Mg_s in Fig. 5(a), just the accumulation regions of orbital electrons appears around the surface O atoms, which indicates that the hybridization effects between N and Mg_s is very weak. For the surface with N adsorbed on Mg_s in Fig. 5(b), both the depletion and accumulation regions of orbital electrons are also found around the O_s atom, which means that the adsorbed N atom would like to bond to the O_s atom while other surface O atoms (surrounding by the

accumulation regions of orbital electrons) prefer to gain electrons from the adsorbed N atom. For the surface with N adsorbed on the interstice in Fig. 5(c), it is obvious that the depletion regions of orbital electrons can be seen around the two O_s atoms nearest the adsorbed N, which results from the surface distortions caused by N adsorption as shown in Figs. 3(c) and 3(f). More importantly, all of above suggests that electron transfer from the adsorbed N to the surface increases gradually from $N_{ads}-Mg_s$ to $N_{ads}-O_s$ and then N_{ads} -interstice, which is consistent with the change trend of hybridization effects between $2p$ electron states of N and O_s in the valance band region as presented in Fig. 4. These results means that the N-induced electron states in N-adsorbed surfaces in Fig. 3 mainly come from the electron transfer from the adsorbed N to the surface, which implies that the catalytic activity of N-adsorbed surface is superior to that of the pure oxide surface [9, 10].

IV. CONCLUSION

The atomic N adsorption effects on electronic structures of MgO(001) surface are investigated by using PWPP-GGA calculations based on the density functional theory. After surfaces relaxations, it is found that both the stability of the adsorbed N atom and surface distortions are deeply dependent on the N atomic position on the surface. The energetically favorable site for atomic N adsorption is the interstices on the surface layer, and the adsorbed N atom prefers to bond to the surface O atoms. From the analysis of the energy band structures, PDOSs and electron densities difference of the surface atoms, it is revealed that the unoccupied electron states caused by atomic N adsorption are closely related to electron transfer from the adsorbed N to the surface, which improves the catalytic activity of the pure surface.

REFERENCES

- [1] J. Graciani, A. Nambu, J. Evans, J. A. Rodriguez, J. F. Sanz. (2008) "Au \leftrightarrow N Synergy and N-Doping of Metal Oxide-Based Photocatalysts", *J. Am. Chem. Soc.*, *36(130)*12056-12603.
- [2] X. R. Wang, X. L. Li, L. Zhang, Y. Yoon, P. K. Weber, H. L. Wang, J. Guo, H. J. Dai. (2009) "N-Doping of Graphene Through Electrothermal Reactions with Ammonia", *Science*, *324(5298)*768-771.
- [3] Y. Y. Mi, S. J. Wang, J. W. Chai, J. S. Pan, C. H. A. Huan, Y. P. Feng, C. K. Ong. (2006) "Effect of Nitrogen doping on optical properties and electronic structures of SrTiO₃ film", *Appl. Phys. Lett.*, *89(23)* 231922.
- [4] I. Marozau, A. Shkabko, G. Dinescu, M. Döbeli, T. Lippert, D. Logvinovich, M. Mallepell, A. Weidenkaff, A. Wokaun, and C. W. Schneider. (2009) "Pulsed laser deposition and characterization of nitrogen-substituted SrTiO₃ thin films", *Appl. Surf. Sci.*, *255(10)*5252-5255.
- [5] C. M. Liu, H. Q. Gu, X. Xiang, Y. Zhang, Y. Y. Jiang, M. Chen, X. T. Zu. (2011) "Optical and magnetic properties of nitrogen ion implanted MgO single crystal", *Chin. Phys. B*, *20(4)*047505.
- [6] N. H. Nickel, M. A. Gluba. (2009) "Defects in Compound Semiconductors Caused by Molecular Nitrogen", *Phys. Rev. Lett.*, *103(14)* 145501.
- [7] M. Pesci, F. Gallino, C. D. Valentin, G. Pacchioni. (2010) "Nature of Defect States in Nitrogen-Doped MgO", *J. Phys. Chem. C*, *114(2)* 1350-1356.
- [8] D. Kim, J. H. Yang, and J. Hong. (2010) "Ultrathin half metallic N and antiferromagnetic semiconducting C layers on MgO(001)", *J. Phys.: Condens. Matter*, *22(48)*486006.

- [9] J. Graciani, L. J. Alvarez, J. A. Rodriguez, J. F. Sanz. (2008) "N Doping of Rutile TiO₂(110) Surface. A Theoretical DFT Study", *J. Phys. Chem. C*, *112*(7) 2624-2631.
- [10] K. L. Zhao, D. Chen, and D. X. Li. (2010) "Effects of N adsorption on the structural and electronic properties of SrTiO₃(001) surface" *Appl. Surf. Sci.*, *256*(12) 6262-6268.
- [11] L. J. Xu, and G. Henkelman. (2008) "Calculations of Ca adsorption on a MgO(100) surface: Determination of the binding sites and growth mode", *Phys. Rev. B*, *77*(20)998-1002.
- [12] P. Frondelius, and H. Häkkinen, and K. Honkala. (2007) "Adsorption of small Au clusters on MgO and MgO/Mo: the role of oxygen vacancies and the Mo-support", *New J. Phys.*, *9*, 339.
- [13] M. D. Segall, P. J. D. Lindan, M. J. Probert, C. J. Pickard, P. J. Hasnip, S. J. Clark and M. C. Payne. (2002) "First-principles simulation: ideas, illustrations and the CASTEP code", *J. Phys.: Cond. Matter.*, *14*(11)2717-2744.
- [14] D. C. Langreth and J. P. Perdew. (1980) "Theory of Non-Uniform Electronic Systems: I. Analysis of the Gradient Approximation and a Generalization that Works", *Phys. Rev. B*, *21*(12) 5469-5493.
- [15] J. P. Perdew, and Y. Wang. (1986) "Accurate and Simple Density Functional for the Electronic Exchange Energy: Generalized Gradient Approximation", *Phys. Rev. B*, *33*(12)8800-8802.
- [16] J. P. Perdew, and S. R. Chevary. (1992) "Atoms, Molecules, Solids, and Surfaces: Applications of the Generalized Gradient Approximation for Exchange and Correlation", *Phys. Rev. B*, *45* 6671-6687.
- [17] M. Marlo and V. Milman. (2000) "Density-functional study of bulk and surface properties of titanium nitride using different exchange-correlation functionals", *Phys. Rev. B*, *62*(4) 2899-2907.
- [18] H. J. Monkhorst, and J. D. Pack. (1976) "Special points for Brillouin-zone integrations", *Phys. Rev. B*, *13*(12) 5188-5192.
- [19] M. C. Payne, M. P. Teter, T. A. Arias, J. D. Joannopoulos. (1992) "Iterative minimization techniques for ab initio total-energy calculations: molecular dynamics and conjugate gradients", *Rev. Mod. Phys.*, *64*(4) 1045-1097.
- [20] D. Vanderbilt. (1990) "Soft self-consistent pseudopotentials in a generalized eigenvalue formalism", *Phys. Rev. B*, *41*(11) 7892-7895.
- [21] P. Pulay. (1969) "Ab initio calculation of force constants and equilibrium geometries in polyatomic molecules", *Mol. Phys.*, *18*(2) 473-480.
- [22] O. L. Anderson, and P. A. Jr. (1966) "Pressure Derivatives of Elastic Constants of Single-Crystal MgO at 23° and -195.8°C", *J. Am. Ceram. Soc.*, *49*(8) 404-409.
- [23] R. C. Whited, C. J. Flaten, W. C. Walker. (1973) "Exciton thermo-reflectance of MgO and CaO", *Solid State Comm.*, *13*(11)1903-1905.
- [24] A. N. Baranov, V. S. Stepanyuk, W. Hergert, et al. (2002) "Full-potential KKR calculations for MgO and divalent impurities in MgO", *Phys. Rev. B*, *66*(15)155117.
- [25] U. Schöberger, and F. Aryasetiawan. (1995) "Bulk and surface electronic structures of MgO", *Phys. Rev. B*, *52*(12) 8788-8793.
- [26] H. Baltache, R. Khenata, M. Sahnoun, M. Driz, B. Abbar, B. Bouhafs. (2004) "Full potential calculation of structural, electronic and elastic properties of alkaline earth oxides MgO, CaO and SrO", *Physica B*, *344*(1-4), 334-342.



Ke-Lun Zhao was born in 27th September 1975. He received doctoral degree from Institute of Metal Research, Chinese Academy of Sciences in 2005-2010. After that he involved on microwave dielectric ceramics in application of mobile communication as a post-doctoral in Harbin Institute of Technology, and then he was Director of R&D in Shenzhen TAT FOOK Technology Co., LTD in 2010-2013. Currently, his main research is focus on the surface modification of metal matrix composite and computational material science as a post-doctoral in School of Mechanical and Automotive Engineering, South China University of Technology.

AUTHORS' PROFILES



Li-Min Fang was born in 20th August 1975. She received B S degree from the School of Physics and Electronic Information Technology of Yunnan Normal University in 2004-2006. After that she has been a lecturer at Department of Physics, Guangdong University of Education until now. Her current research is focus on theoretical physics and computational material science. email id: lmfang1975@163.com